BENTHAM OPEN

CrossMark

The Open Mechanical Engineering Journal

RESEARCH ARTICLE

The Dynamics of One Way Coupling in a System of Nonlinear Mathieu Equations

Alexander Bernstein[1], Richard Rand[2,*] and Robert Meller[3]

[1]*Center for Applied Mathematics, Cornell University, Ithaca, NY 14850, USA*

[2]*Dept. of Mathematics and Dept. of Mechanical and Aerospace Engineering, Cornell University, Ithaca, NY 14850, USA*

[3]*Cornell Lab for Accelerator-based Sciences and Education, Cornell University, Ithaca, NY 14850, USA*

Abstract:

Background:

This paper extends earlier research on the dynamics of two coupled Mathieu equations by introducing nonlinear terms and focusing on the effect of one-way coupling. The studied system of n equations models the motion of a train of n particle bunches in a circular particle accelerator.

Objective:

The goal is to determine (a) the system parameters which correspond to bounded motion, and (b) the resulting amplitudes of vibration for parameters in (a).

Method:

We start the investigation by examining two coupled equations and then generalize the results to any number of coupled equations. We use a perturbation method to obtain a slow flow and calculate its nontrivial fixed points to determine steady state oscillations.

Results:

The perturbation method reveals the existence of an upper bound on the amplitude of steady state oscillations.

Conclusion:

The model predicts how many bunches may be included in a train before instability occurs.

Keywords: Parametric vibrations, Coupled oscillators, Mathieu's equation, Synchrotron, Bifurcation theory, Perturbation methods.

1. INTRODUCTION

In this paper, we investigate the dynamics of the following system of *n* nonlinear Mathieu equations:

$$\ddot{x}_1 + (\delta + \epsilon \cos t)x_1 + \epsilon\gamma x_1^3 + \epsilon\mu\dot{x}_1 \quad = \quad 0 \tag{1}$$

$$\ddot{x}_i + (\delta + \epsilon \cos t)x_i + \epsilon\gamma x_i^3 + \epsilon\mu\dot{x}_i \quad = \quad \epsilon\alpha x_{i-1} \quad , \quad 2 \leq \mathrm{i} \leq n \tag{2}$$

* Address correspondence to this author at the Dept. of Mathematics, Cornell University, Ithaca, NY 14850, USA; Tel: 607 255 8198; E-mails: rhr2@cornell.edu, rrand1@twcny.rr.com

The Mathieu equation is a Hill equation with only one harmonic mode and is an example of parametric excitation. Parametric excitation has been well studied in general [1 - 2], and the Mathieu equation has been well studied in particular [3 - 5]. One of its most salient features is that it has an infinite number of tongues of instability that grow out of the points $\delta = \frac{n^2}{4}$ in the δ - ε plane, where *n* is an integer. As *n* gets larger, the size of each tongue gets narrower, and so the most significant tongue is the one at $\delta = \frac{1}{4}$. This tongue corresponds to a 2:1 subharmonic resonance, and shall be the focus of this paper.

The effect of nonlinearity is to limit the growth of trajectories around the instability; instead of trajectories spiraling towards infinity, they tend towards a stable limit cycle. Of particular interest here is the amplitude of the limit cycle and how that amplitude depends on the various parameters in the problem.

We will investigate the effect of one-way coupling on nonlinear Mathieu equations in this paper. In particular, we will demonstrate that when the amplitude of the coupling coefficient, α, is small enough, the coupled oscillators (2) can have multiple steady state oscillations, and one of these is smaller than the steady state of the uncoupled oscillator (1). When α is large enough, there is only one possible steady state oscillation. In all cases, the sizes of the limit cycles are bound by an upper bound.

It should be noted that this work is based on the assumption that the forcing frequency is constant. The case where the forcing frequency changes as the system spins up has been treated in a recent paper [6] where it was shown that the system can pass through a resonance tongue without excessive growth if the passage is reasonably fast and the tongue is sufficiently narrow.

Our interest in Eqs.(1, 2) comes from an application in the design of particle accelerators.

1.1. Application

This work was motivated by a novel application in particle physics, namely the dynamics of a generic circular particle accelerator. Since this application is expected to be unfamiliar to most readers of this journal, we offer the following description of a synchrotron [7].

The synchrotron is a particle accelerator in which a "Particle" actually consists of a group of electrons called a "Bunch," and the collection of all bunches is called a "Train." We ignore the interactions of electrons inside each bunch and treat the entire bunch as a single particle.

Each bunch leaves an electrical disturbance behind it as it traverses around the synchrotron, and these wake fields are the main source of coupling in the model. The coupling is mediated by several sources, including ion coupling and the electron cloud effect.

Particle paths in the synchrotron are circle-like but are not exact circles. Since the synchrotron lacks a central force, the circle-like particle orbits are achieved through the use of about 100 electromagnets spread around the periphery Fig. (**1**).
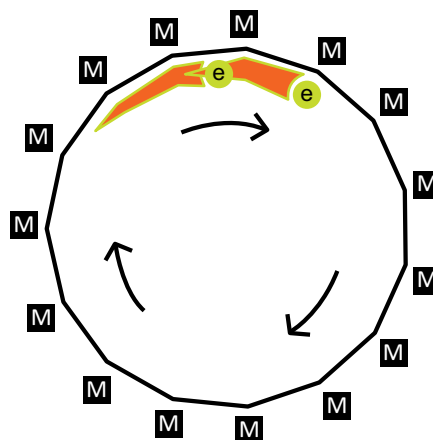
Fig. (1). Two bunches moving clockwise along a polygonal path through the use of a system of electromagnets.

This means that the magnetic external forcing is periodic in rotation angle θ; assuming that the angular velocity of the bunch is constant with $\theta = \omega t$, the forcing is periodic in time as well. We can express this forcing function as a Fourier series, and we shall approximate this series by the first couple of terms in it, namely the constant term and the first cosine term.

We model each bunch as a scalar variable $x_i(t)$, $i = 1,...,n$. Here, x_i is the vertical displacement above equilibrium of the center of mass of the ith bunch. Each x_i is modeled as a damped parametrically-forced oscillator, and we write:

$$\ddot{x}_1 + (\delta + \epsilon \cos t)x_1 + \epsilon \gamma x_1^3 + \epsilon \mu \dot{x}_1 = 0$$
$$\ddot{x}_i + (\delta + \epsilon \cos t)x_i + \epsilon \gamma x_i^3 + \epsilon \mu \dot{x}_i = \epsilon \alpha x_{i-1} \ , \quad 2 \leq i \leq n$$

The nonlinear terms are included to create a more realistic model since most natural phenomena are nonlinear and linear models are a convenient approximation. The nonlinear parameter, γ, can be chosen to adjust the scale of the problem.

The damping terms are also included to create a more realistic model.

The coupling terms on the right-hand side may be viewed as the strength of the plasma interactions: the radiation from a bunch produces an electron cloud which travels behind the bunch. This radiation dissipates away very quickly though, and so this coupling has a short range and can only influence the dynamics of the next bunch in the train. The coupling strength is affected by both the spacing between bunches as well as the charge of each bunch, and α encapsulates both of those effects.

2. TWO-VARIABLE EXPANSION

We use the two-variable expansion method [8, 9] to study the dynamics of Eqs. (1, 2). We set

$$\xi(t) = t, \quad \eta(t) = \epsilon t$$

where ξ is the time t and η is the slow time.

Since the x_i terms are functions of ξ and η, the derivative with respect to time t is expressed through the chain rule:

$$\dot{x}_i = x_{i_\xi} + \epsilon x_{i_\eta}, \quad 1 \leq i \leq n$$

Similarly, for the second derivative we obtain:

$$\ddot{x}_i = x_{i_{\xi\xi}} + 2\epsilon x_{i_{\xi\eta}} + \epsilon^2 x_{i_{\eta\eta}}, \quad 1 \leq i \leq n$$

In this paper, we only perturb up to $O(\varepsilon)$, and so we will ignore the ε^2 terms.

We then expand the x_i terms in a power series in ε:

$$x_i(\xi, \eta) = x_{i_0}(\xi, \eta) + \epsilon x_{i_1}(\xi, \eta) + O(\epsilon^2), \quad 1 \leq i \leq n \tag{3}$$

In addition, we detune off the 2:1 subharmonic resonance by setting:

$$\delta = \frac{1}{4} + \epsilon \delta_1 + O(\epsilon^2) \tag{4}$$

Substituting (3), (4) into (1), (2) and collecting terms in ε, we arrive at the following equations:

$$x_{i_{0,\xi\xi}} + \frac{1}{4}x_{i_0} = 0, \quad 1 \leq i \leq n \tag{5}$$

$$x_{i_{1,\xi\xi}} + \frac{1}{4}x_{i_1} = -2x_{i_{0,\xi\eta}} - \gamma x_{i_0}^3 - \mu x_{i_0,\xi} - \delta_1 x_{i_0} - x_{i_0} \cos \xi, \quad 1 \leq i \leq n \tag{6}$$

The solution to (5) is simply:

$$x_{i_0} = A_i(\eta) \cos\left(\frac{\xi}{2}\right) + B_i(\eta) \sin\left(\frac{\xi}{2}\right), \quad 1 \le i \le n \tag{7}$$

We then substitute (7) into (6). Using trigonometric identities, these equations can be written in terms of $\cos\frac{\xi}{2}$ and $\sin\frac{\xi}{2}$. We set the coefficients of such terms equal to zero in order to remove the secular terms which cause resonance. This results in 2*n* equations in 2*n* unknowns:

$$A_1' = -\frac{B_1}{2} + \delta_1 B_1 - \frac{\mu A_1}{2} + \frac{3\gamma}{4} B_1(A_1^2 + B_1^2) \tag{8}$$

$$B_1' = -\frac{A_1}{2} - \delta_1 A_1 - \frac{\mu B_1}{2} - \frac{3\gamma}{4} A_1(A_1^2 + B_1^2) \tag{9}$$

$$A_i' = -\frac{B_i}{2} + \delta_1 B_i - \frac{\mu A_i}{2} + \frac{3\gamma}{4} B_i(A_i^2 + B_i^2) - \alpha B_{i-1}, \quad 2 \le i \le n \tag{10}$$

$$B_i' = -\frac{A_i}{2} - \delta_1 A_i - \frac{\mu B_i}{2} - \frac{3\gamma}{4} A_i(A_i^2 + B_i^2) + \alpha A_{i-1}, \quad 2 \le i \le n \tag{11}$$

These equations are known as the slow flow of the system and represent the envelope of the oscillatory motion of equations (1, 2). Finding the equilibrium points of the slow flow is analogous to finding simple harmonic motion with constant amplitude in the original system. In doing so, we will not only obtain information on the amplitude of these limit cycles but also information on where Hopf bifurcations occur in parameter space.

3. ANALYTIC RESULTS

3.1. The First Bunch

The dynamics of the first bunch are given by eqs. (8, 9).

$$A_1' = -\frac{B_1}{2} + \delta_1 B_1 - \frac{\mu A_1}{2} + \frac{3\gamma}{4} B_1(A_1^2 + B_1^2)$$

$$B_1' = -\frac{A_1}{2} - \delta_1 A_1 - \frac{\mu B_1}{2} - \frac{3\gamma}{4} A_1(A_1^2 + B_1^2)$$

As this system is 2-dimensional, the complete dynamics can be expressed in the phase plane A_1-B_1. The Numerical Results section contains various graphs demonstrating the full dynamics of the first bunch, but the rest of this section will focus purely on calculating the equilibrium points of the system.

Setting these equations equal to zero gives us the following equilibrium points:

$$(A_1^*, B_1^*) = (0,0), \quad \left(0, \pm\sqrt{\frac{\pm\sqrt{1-\mu^2}(2\delta_1-1) - \mu^2 + 1 - 2\delta_1}{3\gamma}}\right), \quad \left(\pm\sqrt{\frac{\pm\sqrt{1-\mu^2}(2\delta_1+1) + \mu^2 - 1 - 2\delta_1}{3\gamma}}, 0\right)$$

Here, we use the standard notation A_i^*, B_i^* to denote equilibrium points of the variables A_i, B_i.

To simplify matters, we will focus on the special case when $\delta_1 = 0$ and $\mu = 0$. Setting $\delta_1 = 0$ lets us examine the point of resonance directly without considering points in the neighborhood of the resonance, and setting $\mu = 0$ ignores the effects of damping which ends up having a negligible effect on the analysis of the steady state. The fixed points in this case are:

$$(A_1^*, B_1^*) = (0,0), \quad \left(0, \pm\sqrt{\frac{2}{3\gamma}}\right), \quad \left(\pm i\sqrt{\frac{2}{3\gamma}}, 0\right) \tag{12}$$

Here, we note our first major observation: Nontrivial real equilibrium points for A_1 only exist for $\gamma < 0$, and nontrivial real equilibrium points for B_1 only exist for $\gamma > 0$. However, the magnitude of the amplitude is the same in both cases, and the analysis of both cases is identical. Without the loss of generality, we will take $\gamma > 0$ and $A_1^* = 0$.

3.2. The Second Bunch

The dynamics of the second bunch are given when $i = 2$ in eqs. (10, 11).

$$A_2' \;=\; -\frac{B_2}{2} + \delta_1 B_2 - \frac{\mu A_2}{2} + \frac{3\gamma}{4} B_2(A_2^2 + B_2^2) - \alpha B_1 \tag{13}$$

$$B_2' \;=\; -\frac{A_2}{2} - \delta_1 A_2 - \frac{\mu B_2}{2} - \frac{3\gamma}{4} A_2(A_2^2 + B_2^2) + \alpha A_1 \tag{14}$$

Note that these equations share a similar structure to eqs. (8 and 9) but with additional terms resulting from the one-way coupling. These additional terms mean the dynamics of the second bunch are 4-dimensional instead of 2-dimensional like the first bunch, and we cannot view the dynamics in a phase plane. Our analysis of the second bunch will focus only on the steady-state solutions and not on the general dynamics.

Since we are taking $\gamma > 0$, all equilibrium points for the first bunch require $A_1^* = 0$; substituting $A_1^* = 0$ into eqs. (13, 14) yields:

$$\frac{B_2^*[3\gamma(A_2^{*^2} + B_2^{*^2}) - 2] - 4\alpha B_1^*}{4} \;=\; 0 \tag{15}$$

$$\frac{A_2^*[3\gamma(A_2^{*^2} + B_2^{*^2}) + 2]}{4} \;=\; 0 \tag{16}$$

Note that $A_2^{*^2} + B_2^{*^2}$ is a nonnegative value, and is only identically zero in the trivial solution $(A_2^{*^2}, B_2^{*^2}) = (0,0)$. Since we are interested in nontrivial solutions, we require that $A_2^{*^2} + B_2^{*^2}$ be positive.

However, since $\gamma > 0$, the expression $3\gamma(A_2^{*^2} + B_2^{*^2}) + 2$ must be positive. Thus, the only way for (16) to equal zero is for $A_2^* = 0$.

Substituting $A_2^* = 0$ into (15) yields:

$$\frac{3\gamma}{4} B_2^{*^3} - \frac{1}{2} B_2^* - \alpha B_1^* = 0 \tag{17}$$

Since B_1^* is already known to us from eq. (12), solving this cubic equation will give us the solution for B_2^*.

This solution gives us the steady-state of B_2. The full dynamics of the system is 4-dimensional, involving A_1, B_1, A_2 and B_2, and cannot be expressed in a phase plane.

A graph of the relationship between B_2^* and α can be seen in Fig. (**2**).

3.3. The Third Bunch

The dynamics of the third bunch are given when $i = 3$ in eqs. (10, 11).

$$A_3' \;=\; -\frac{B_3}{2} + \delta_1 B_3 - \frac{\mu A_3}{2} + \frac{3\gamma}{4} B_3(A_3^2 + B_3^2) - \alpha B_2 \tag{18}$$

$$B_3' \;=\; -\frac{A_3}{2} - \delta_1 A_3 - \frac{\mu B_3}{2} - \frac{3\gamma}{4} A_3(A_3^2 + B_3^2) + \alpha A_2 \tag{19}$$

Note that these equations share the *exact* same structure as eqs. (13, 14). Just like with the second bunch, the presence of additional terms means that the dynamics of the third bunch are 4-dimensional. This means that we can't view the dynamics in a phase plane, and so our analysis of the third bunch will focus only on the steady-state solutions and not on the general dynamics.
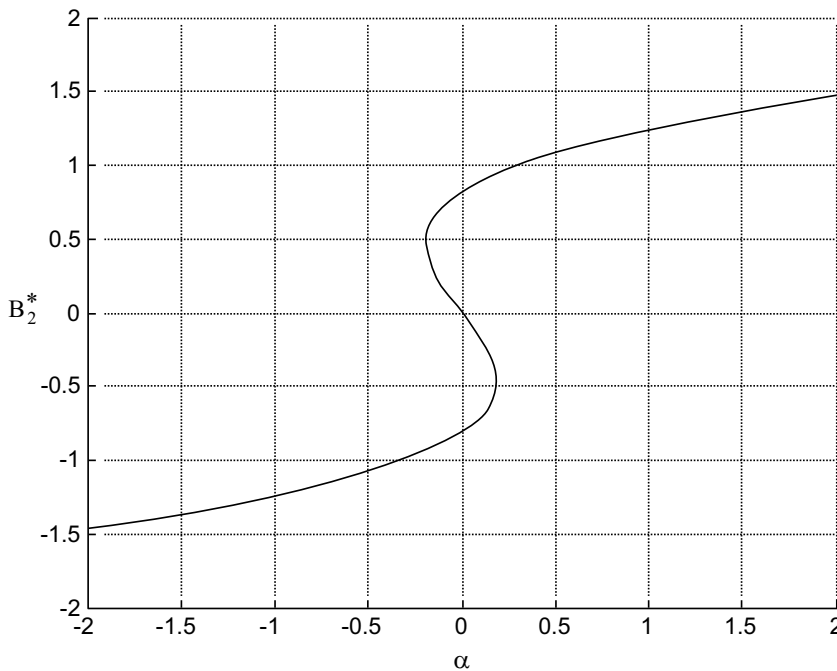
Fig. (2). Plot of B_2^* as a function of α, for $\gamma = 1$ and $B_1^* = \sqrt{\frac{2}{3}}$.

We know from the analysis of the second bunch that $A_2^* = 0$ is necessary for all steady state solutions of the second bunch; substituting $A_2^* = 0$ into eqs. (18, 19) yields:

$$\frac{B_3^*[3\gamma(A_3^{*^2} + B_3^{*^2}) - 2] - 4\alpha B_2^*}{4} \quad = \quad 0 \tag{20}$$

$$\frac{A_3^*[3\gamma(A_3^{*^2} + B_3^{*^2}) + 2]}{4} \quad = \quad 0 \tag{21}$$

Note that $A_3^{*^2} + B_3^{*^2}$ is a nonnegative value, and is only identically zero in the trivial solution (A_3^*, B_3^*) = (0,0). Since, we are interested in nontrivial solutions, we require that $A_3^{*^2} + B_3^{*^2}$ be positive.

However, since $\gamma > 0$, the expression $3\gamma(A_2^{*^2} + B_2^{*^2}) + 2$ must be positive. Thus, the only way for (21) to equal it to zero is for $A_3^* = 0$.

Substituting A_3^* into (20) yields:

$$\frac{3\gamma}{4}B_3^{*^3} - \frac{1}{2}B_3^* - \alpha B_2^* = 0 \tag{22}$$

Since B_2^* is already known to us from eq. (17), solving this cubic equation will give us the solution for B_3^*.

The graph of the relationship between B_3^* and α will look qualitatively similar to the relationship between B_2^* and α Fig. (**2**) but they will differ quantitatively since the value of B_2^* that is substituted into eq. (22) will in general be different than the value of B_1^* that is substituted into eq. (17).

Still, given the similarity between eq. (22 and 17), it is natural to ask if this pattern continues for all later bunches. Indeed, this is the case, and so we will generalize the results found in these past two sections to the nth bunch in the system, where n can be any integer.

3.4. The nth Bunch

Due to the nature of one-way coupling, the dynamics of all the bunches except the first one are identical, as can be seen in the results found for the second and third bunches. Thus, we can easily derive a formula for calculating the steady-state solution for the nth bunch for any $n > 1$:

$$\frac{3\gamma}{4}B_n^{*^3} - \frac{1}{2}B_n^* - \alpha B_{n-1}^* = 0 \tag{23}$$

Unfortunately, calculating B_n^* in practice requires calculating the amplitudes of *all* bunches in front of it, since the recursive relationship cannot be simplified into a formula dependent only on the first bunch. Part of the problem is that each step requires solving a cubic equation which, although solvable in principle, is a tangled mess. In practice, it is much easier to use numerical root solving methods to find the amplitudes for all the bunches.

The other, bigger problem is that cubic equations have three roots; if all three roots are real and distinct, then we have a multi-valued function. Fortunately, this only occurs for a range of α values, and we can easily determine this region through analytic means.

3.5. Multi-Valued Regions

Note that in Fig. (**2**), there are two points with infinite slope: these are the points that divide the function into multi-valued regions and single-valued regions. If we flipped the two axes, then these two points change from having infinite slope to zero slopes see Fig. (**3**). Thus, we want to derive $\frac{d\alpha}{dB_n^*}$ and find the values of α for which the derivative is equal to zero.
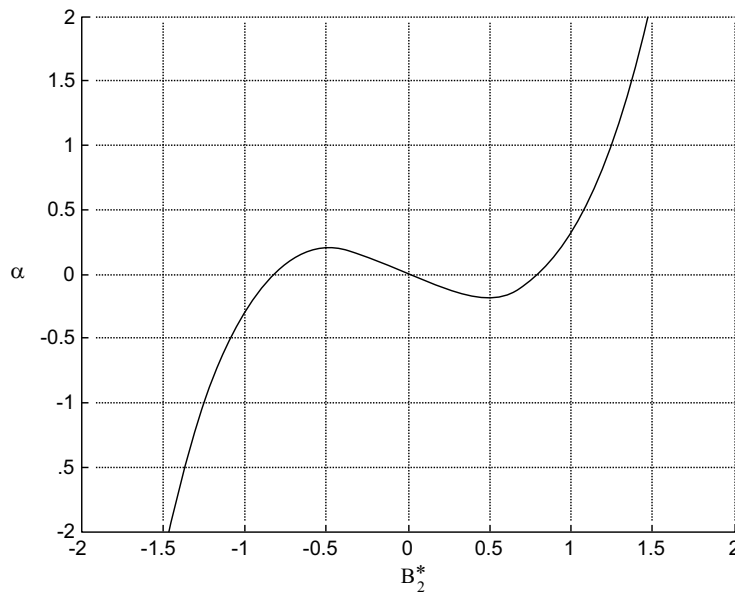
Fig. (3). Plot of α as a function of B_2^*, for $\gamma = 1$ and $B_1^* = \sqrt{\frac{2}{3}}$.

We start by moving the α term in eq. (23) to the right hand side and differentiating both sides.

$$\left(\frac{9\gamma}{4}B_n^{*^2} - \frac{1}{2}\right)dB_n^* = B_{n-1}^* d\alpha$$

Here B_{n-1}^* is a constant since we're assuming all B_i^* up to $i = n$ - 1 have already been found.

Solving for $\frac{d\alpha}{dB_n^*}$, we obtain:

$$\frac{d\alpha}{dB_n^*} = \frac{1}{B_{n-1}^*}\left(\frac{9\gamma}{4}B_n^{*^2} - \frac{1}{2}\right)$$

We set this equal to zero to find the local extrema:

$$\frac{9\gamma}{4}B_n^{*2} - \frac{1}{2} = 0 \quad \Rightarrow \quad B_n^* = \pm\sqrt{\frac{2}{9\gamma}}$$

Finally, we substitute this result into eq. (23) to find the corresponding α value:

$$B_{n-1}^*\alpha = \left(\frac{3\gamma}{4}\left(\frac{2}{9\gamma}\right) - \frac{1}{2}\right)\left(\pm\sqrt{\frac{2}{9\gamma}}\right) \quad \Rightarrow \quad \alpha = \pm\frac{1}{B_{n-1}^*}\sqrt{\frac{2}{81\gamma}} \tag{24}$$

One important feature of this result is that the range of α values for the nth bunch depends on the bunch before it. As an example, for B_2^*, the α range depends on $B_1^* = \sqrt{\frac{2}{3\gamma}}$; multiple limit cycles are possible for B_2^* when $\alpha \in [-3^{-3/2}, 3^{-3/2}] \approx (-0.2, 0.2)$.

The significance of this result is that fixing α does *not* guarantee that *all* bunches B_i^* will be either multi-valued or single valued; it is possible to choose α such that B_2^* only has one limit cycle, but B_3^* has three.

A natural question to ask at this point is whether there exist values of α that *do* guarantee single valuedness for all B_i^*. Due to the relationship of eq. (24), a uniform bound on α requires a uniform bound on B_i^*, so this question is equivalent to asking if there is a bound on how large B_i^* can become.

3.6. Limit as n → ∞

It turns out that the B_i^* are indeed bound by an upper bound, and this can be shown by examining the limit as $n \to \infty$.

In particular, we care about the limit of the amplitude $|B_n^*|$. One way for this limit to exist is if $B^* = B_n^* = B_{n-1}^*$ as $n \to \infty$. In this case, each bunch has the same amplitude as the bunch before it, and each bunch is oscillating in phase with the bunch before it.

By setting $B^* = B_{n-1}^* = B_n^*$ in eq. (23), we obtain:

$$B^*\left(\frac{3\gamma}{4}B^{*2} - \frac{1}{2} - \alpha\right) = 0 \tag{25}$$

Thus, we find that the possible in-phase limits are:

$$B^* = 0, \quad \pm\sqrt{\frac{2(1+2\alpha)}{3\gamma}} \tag{26}$$

As long as $\alpha \geq -1/2$, these three limits are distinct; otherwise, no in-phase limit cycles are possible.

Another possibility is to examine the case when $B^* = B_n^* = B_{n-1}^*$ as $n \to \infty$. In this case, each bunch has the same amplitude as the bunch before it, and each bunch is oscillating 180 degrees out of phase with the bunch before it.

By setting $B^* = B_{n-1}^* = -B_n^*$ in eq. (23), we obtain:

$$B^*\left(\frac{3\gamma}{4}B^{*2} - \frac{1}{2} + \alpha\right) = 0 \tag{27}$$

Thus, we find that the possible limits are:

$$B^* = 0, \quad \pm\sqrt{\frac{2(1-2\alpha)}{3\gamma}} \tag{28}$$

As long as $\alpha \leq 1/2$, these three limits are distinct; otherwise, no out-of-phase limit cycles are possible.

Therefore, in the limit as $n \to \infty$, there are three possible cases:

- For $\alpha < -1/2$, only out-of-phase limit cycles can exist.

- For $-1/2 < \alpha < 1/2$, both out-of-phase and in-phase limit cycles can exist.
- For $1/2 < \alpha$, only in-phase limit cycles can exist.

Fig. (**4**) shows the upper bound for both types of limit cycles.
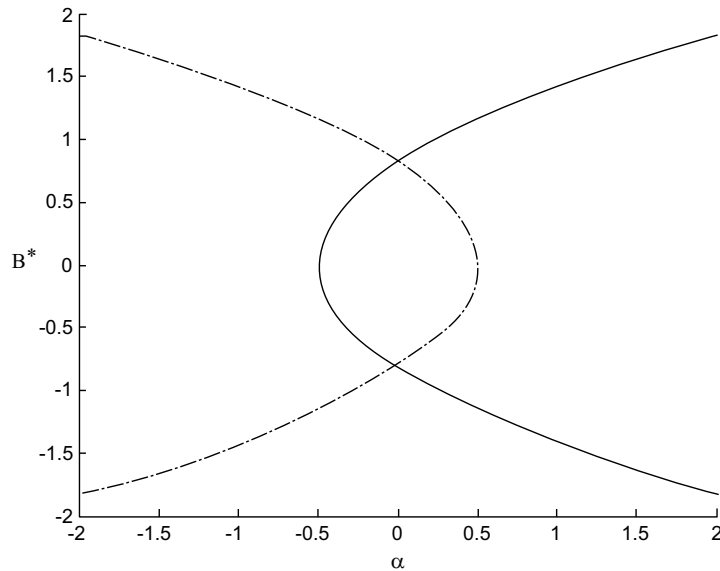
Fig. (4). The solid curve is the upper bound on amplitude of the in-phase limit cycle. The dashed-dot curve is the upper bound on the amplitude of the out-of-phase limit cycle.

4. NUMERICAL RESULTS

4.1. Phase Plane

To help visualize the dynamics of the first bunch, graphs showing the phase plane for eqs. (8 and 9) are provided below. All phase plane graphs were made using PPLANE [10].

Fig. (**5**) compares the cases when $\gamma > 0$ and $\gamma < 0$. Qualitatively, the graphs are the same; the only difference is that one has the equilibrium points on the A axis and the other has the equilibrium points on the B axis.

Fig. (**6**) shows the effect of including small values of δ_l and μ. The inclusion of damping has broken the homoclinic orbit and all orbits are eventually attracted to one of the two stable equilibrium points. Since the two basins of attraction are intertwined, it can be hard in practice to determine which equilibrium point will be reached from a given initial condition.

Fig. (**7**) shows the effect of including larger values of δ_l and μ. The equilibrium points have gone through a pitchfork bifurcation and there is now only one equilibrium point: the origin.

4.2. Cobweb Diagram

Since all bunches other than the first bunch are coupled to another bunch, we cannot express their dynamics in a phase plane. Instead, we will show the amplitudes B_1^* through B_n^* in a cobweb diagram for a fixed number n.

Each diagram contains the graphs of Eq. (23), with B_n^* on the x-axis and B_{n-1}^* on the y-axis, and the line $y = x$. The sequence starts with B_1^* on the x-axis, and proceeds as follows:

- Move vertically to the line $y = x$.
- Move horizontally to the curve given by Eq. (23) [may be multi-valued].
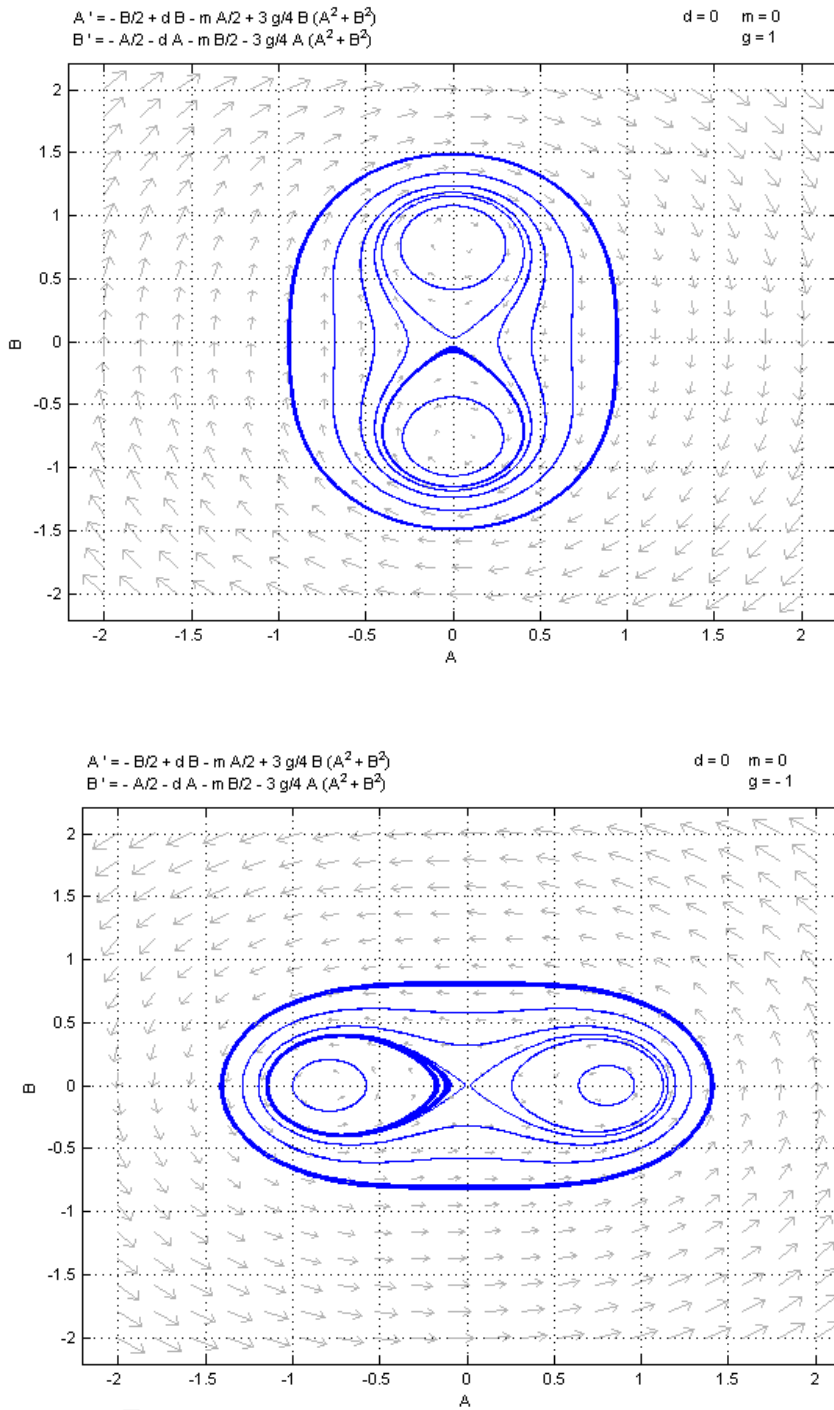
Fig. (5). Phase plots of the A_1-B_1 dynamics. The left plot shows the dynamics for $\gamma = 1$ and the right plot shows the dynamics for $\gamma = -1$. Both plots have $\alpha = 0$ and $\mu = 0$.

A ' = - B/2 + d B - m A/2 + 3 g/4 B (A² + B²)
B ' = - A/2 - d A - m B/2 - 3 g/4 A (A² + B²)

d = .1   m = .1
g = 1
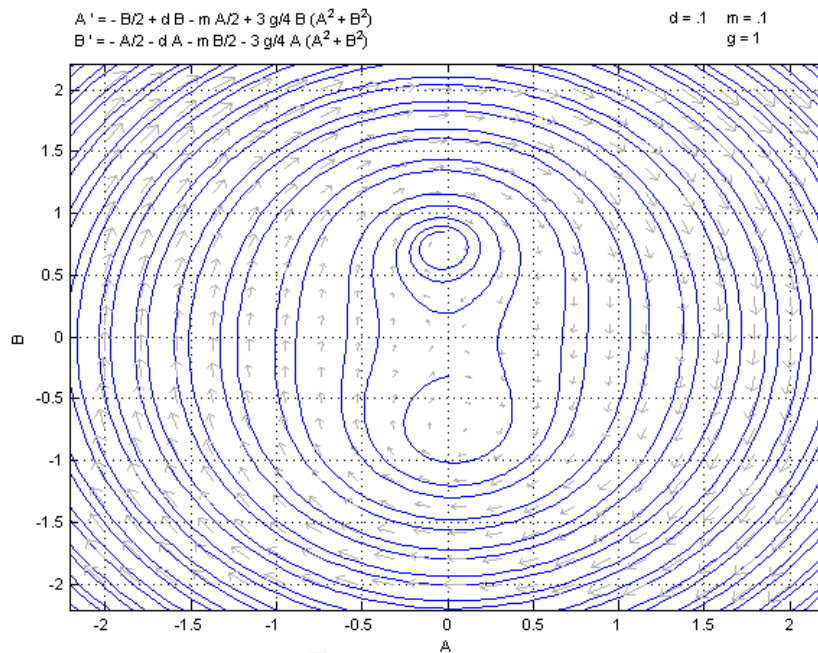
Fig. (6). Phase plot of the A_1-B_1 dynamics. Parameter values are $\alpha = 0.1$, $\mu = 0.1$ and $\gamma = 1$.

A ' = - B/2 + d B - m A/2 + 3 g/4 B (A² + B²)
B ' = - A/2 - d A - m B/2 - 3 g/4 A (A² + B²)

d = 1   m = 1
g = 1
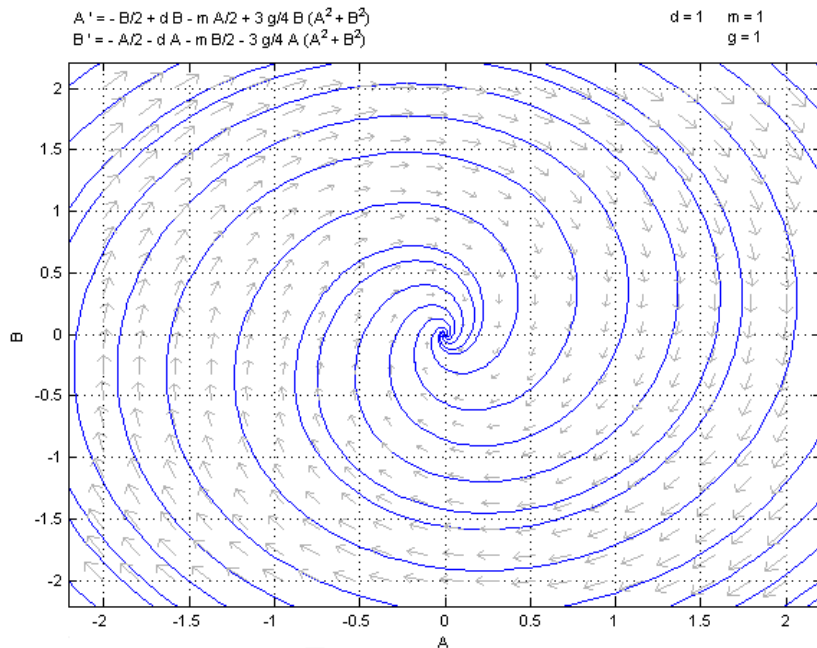
Fig. (7). Phase plot of the A_1-B_1 dynamics. Parameter values are $\alpha = 1$, $\mu = 1$ and $\gamma = 1$.

This process is repeated n times, with each horizontal change determining the next value of B_i^*.

For example, Fig. (**8**) shows the case when $\alpha > 1/2$. The diagram begins at the point (0.8,0), representing the value $B_1^* = \sqrt{2/3}$. After moving up to the line $y = x$ at (0.8,0.8), the process then moves to the right to (1.1,0.8), where 1.1 represents the next value, B_2^*. After several iterations, the values of B_i^* approach the point (1.2,1.2), where 1.2 is the size of the stable limit cycle in this region.
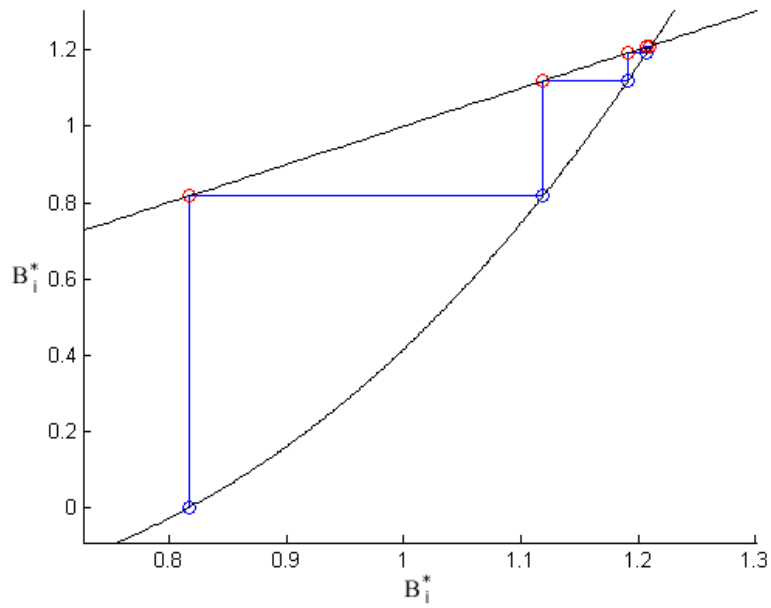
Fig. (8). Cobweb diagram for $\alpha = 0.6$ and $\gamma = 1$.

Fig. (**9**) shows the case when $\alpha < -1/2$. The diagram begins at the point (0.8,0), as before. This time, after moving up to the point (0.8,0.8), the process then moves to the left to (-1.2,0.8), where -1.2 represents the next value, B_2^*. After several iterations, the values of B_i^* alternate between two values, 1.3 and -1.3, reflecting the out-of-phase nature of the stable limit cycle in this region.
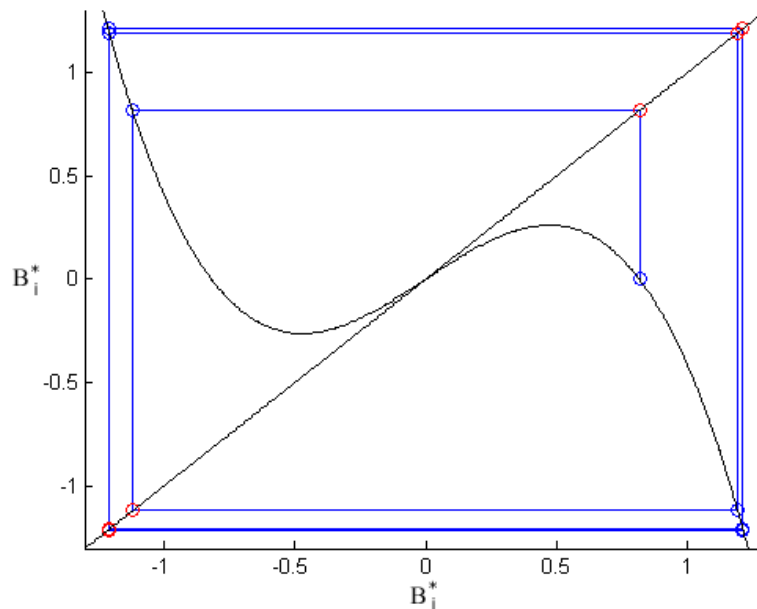
Fig. (9). Cobweb diagram for $\alpha = -0.6$ and $\gamma = 1$.

For $-1/2 < \alpha < 1/2$, there are three possible limit cycles. Since the output of eq. (23) is multi-valued in this region, there are many different cobweb diagrams for a given starting point B_1^*, with the realized outcome determined by the initial condition in the original system (1, 2). The code used to generate the diagrams picks one of the three limit cycles at random, as this best represents the unpredictability of knowing the precise initial condition.

Fig. (**10**) shows the chaotic nature of this iteration map in the region $-1/2 < \alpha < 1/2$. Since the behavior here is randomized, there is no clear pattern to be discerned here. However, we note that the attractor seems to be a fractal of some kind since there are gaps that are never reached.
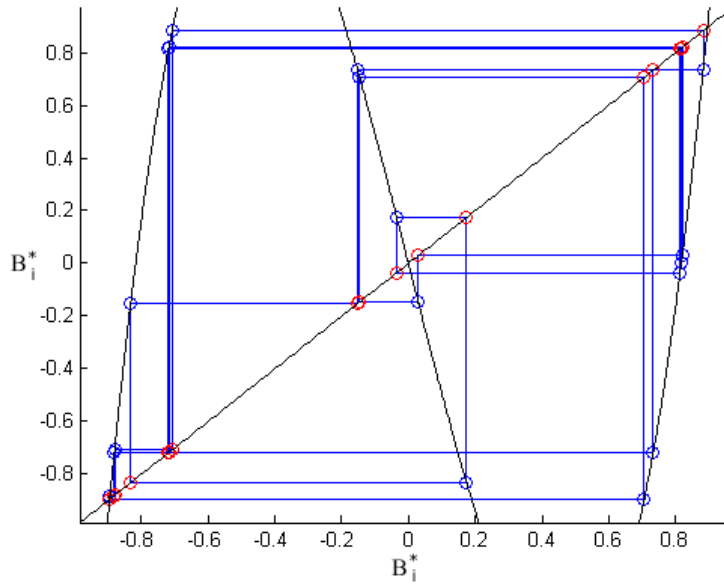
Fig. (10). Cobweb diagram for $\alpha = 0.1$ and $\gamma = 1$.
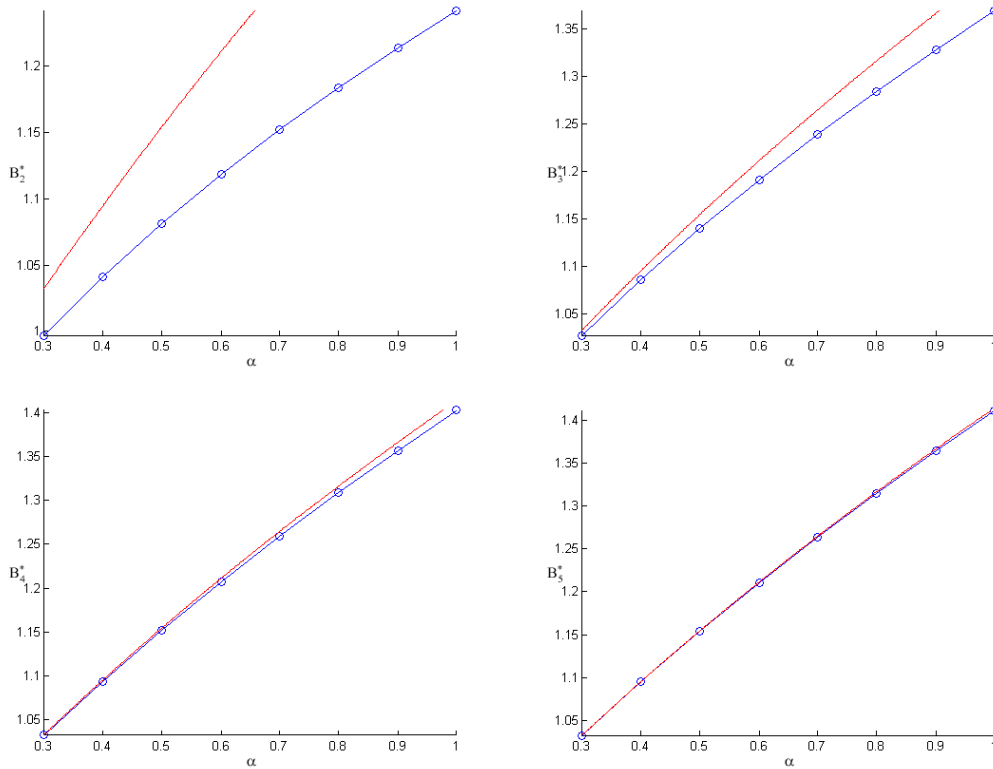
Fig. (11). Plots of B_n^* vs α for $\alpha \geq 0.3$ and $\gamma = 1$. The top left graph shows $n = 2$, the top right graph shows $n = 3$, the bottom left graph shows $n = 4$, and the bottom right graph shows $n = 5$.

4.3. Convergence to the Limit

The most important question in this model is determining how long a train of bunches can be before the tail becomes unstable. We have shown that there is a theoretical upper bound to the limit cycle amplitude, but it remains to be seen how quickly the numerical sequence given by Eq. (23) approaches this limit.

Fig. (**11**) shows a sequence of graphs of B_n^* vs α for $2 \leq n \leq 5$ and $\alpha \geq 0.3$, which demonstrates the speed at which this sequence approaches the limit. However, we note that the sequence does not seem to converge pointwise at the same rate, and for larger α values, it takes longer to converge to the limit.

Fig. (**12**) shows the graph of B_5^* vs α for a larger range of α values, including the multi-valued region. While the multi-valued region does not show convergence to either of the limit curves, the values do stay bounded between the maximum values of the two limit curves. Thus, even in this region we, can place an upper bound on how large the B_i^* can grow.
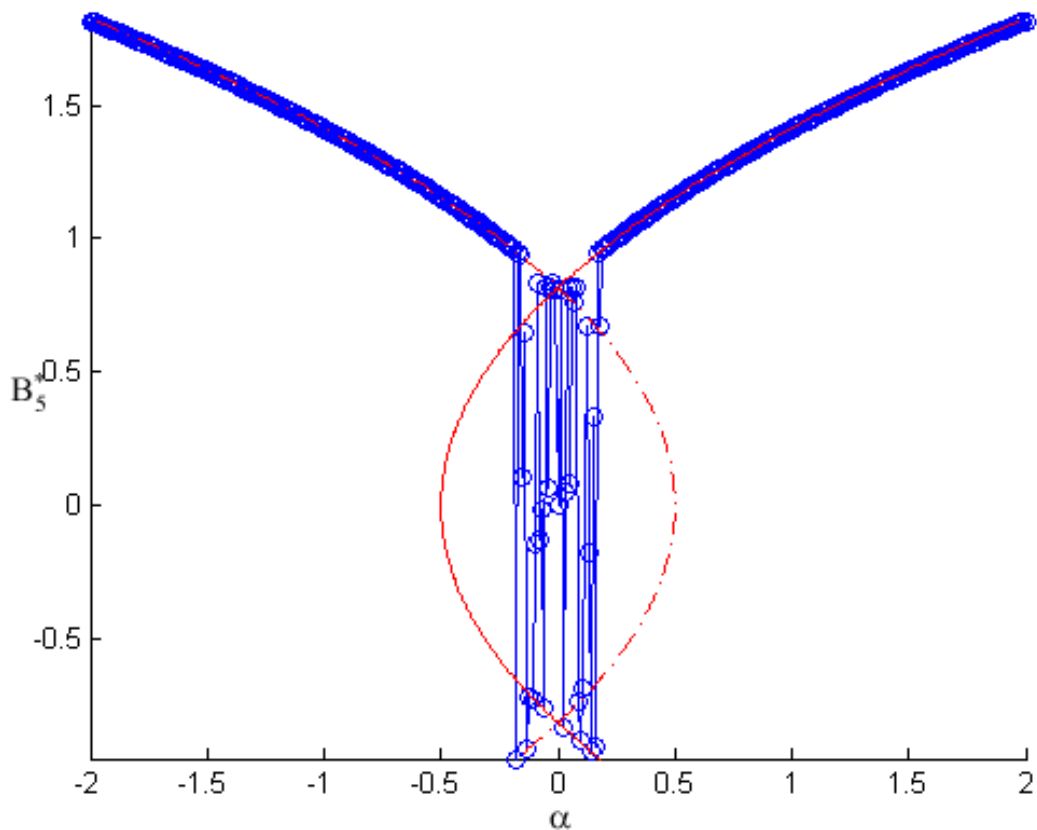
Fig. (12). Plots of B_5^* vs α for -2≤α≤2 and γ = 1.

Fig. (**13**) shows the graph of B_6^* vs α. For $\alpha > 0.5$, this figure is almost identical to Fig. (**12**), but for $\alpha < -0.5$ the sign of the curve is now negative instead of positive. This reflects how the limit cycle in this region is out-of-phase, as B_6^* is out of phase with B_5^*. Since the magnitude of the limit curve is the same for both positive and negative branches, the sign of B_n^* is of little concern.
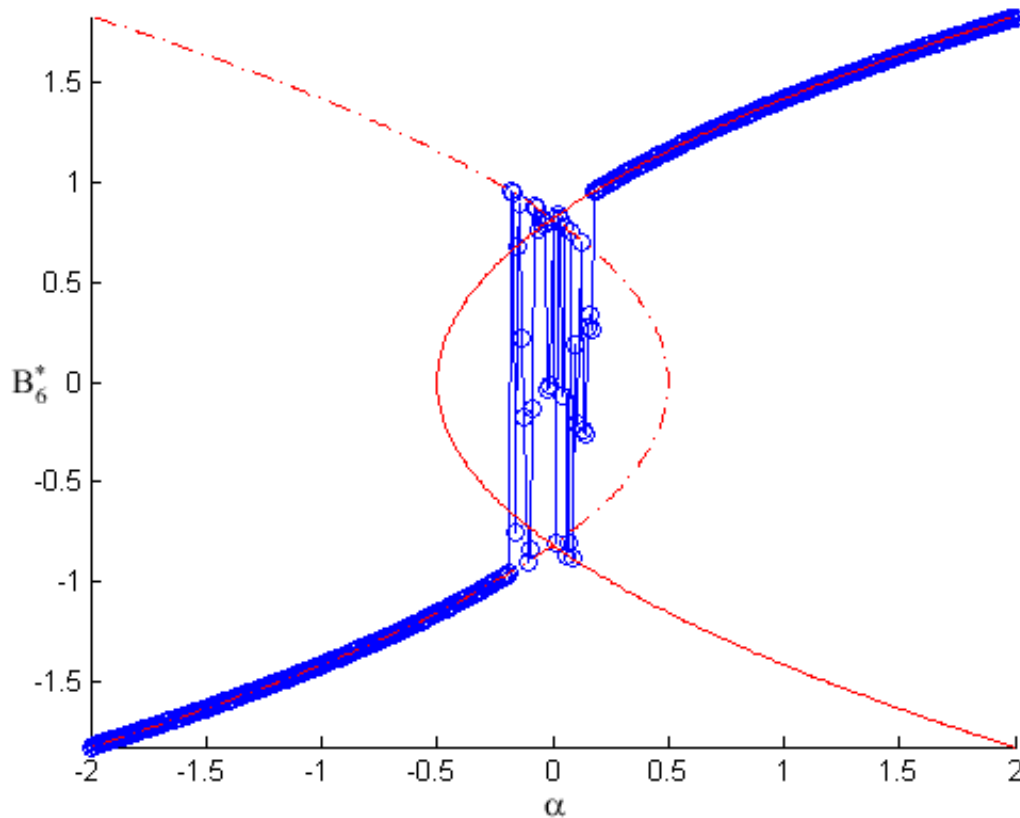
Fig. (13). Plots of B_6^* vs α for $-2 \leq \alpha \leq 2$ and $\gamma = 1$.

CONCLUSION

Our model predicts an upper bound for the amplitudes of bunches in a train. While the dynamics of the system varies depending on the value of α, the upper bound holds for all values of α.

In theory, this means that all trajectories are bounded, but in practice, there is a physical bound on how large amplitudes can grow before they become unstable. For example, if the theoretical bound on the motion is 100 centimeters, but the radius of the cross-section of the accelerator is only 2 centimeters, then instability occurs once B_n^* grows larger than 2 centimeters. On the other hand, if the theoretical bound on the motion is 1 centimeter, then instability will never occur, as B_n^* will never grow larger than 2 centimeters.

If it is known that the physical upper bound is smaller than the theoretical upper bound, then it is a simple matter to numerically calculate B_n^* from eq. (23) and determine at what point B_n^* exceeds the physical bound. Even in the multi-valued region, taking the worst-case scenario when the amplitude grows, the largest at each step will determine the critical n at which instability occurs. Thus, it is possible to know how many bunches to include in a train before instability occurs.

If this model proves accurate, then α can be used to determine the maximum number of bunches in a train. As α contains information for both the per-bunch charge and the per-bunch spacing, adjusting either of these specifications can adjust the value of α, and thus affect the size of the train.

CONSENT FOR PUBLICATION

Not applicable.

CONFLICT OF INTEREST

The authors declare no conflict of interest, financial or otherwise.

ACKNOWLEDGEMENTS

REFERENCES

[1]   J. Cuevas, L.Q. English, P.G. Kevrekidis, and M. Anderson, "Discrete breathers in a forced-damped array of coupled pendula: Modeling, computation, and experiment", *Phys. Rev. Lett.,* vol. 102, no. 22, p. 224101, 2009.
[http://dx.doi.org/10.1103/PhysRevLett.102.224101] [PMID: 19658866]

[2]   M. Syafwan, H. Susanto, and S.M. Cox, "Discrete solitons in electromechanical resonators", *Phys. Rev. E Stat. Nonlin. Soft Matter Phys.,* vol. 81, no. 2 Pt 2, p. 026207, 2010.
[http://dx.doi.org/10.1103/PhysRevE.81.026207] [PMID: 20365638]

[3]   C.S. Hsu, "On a restricted class of coupled Hill's equations and some applications", *J. Appl. Mech.,* vol. 28, no. 4, pp. 551-556, 1961.
[http://dx.doi.org/10.1115/1.3641781]

[4]   A. Bernstein, and R.H. Rand, "Coupled Parametrically Driven Modes in Synchrotron Dynamics", *In: Proceedings of the 33rd IMAC, A Conference and Exposition on Structural Dynamics*, G. Kerschen, Ed., Springer: Newyork, 2016
[http://dx.doi.org/10.1007/978-3-319-15221-9_8]

[5]   I. Kovacic, R.H. Rand, and S.M. Sah, "Mathieu's equation and its generalizations: Overview of stability charts and their features", *Appl. Mech. Rev.,* vol. 70, no. 2, p. 020802, 2018.
[http://dx.doi.org/10.1115/1.4039144]

[6]   G.M. Wang, T. Shaftan, V. Smaluk, Y. Li, and R. Rand, "Lossless crossing of a resonance stopband during tune modulation by synchrotron oscillations", *New J. Phys.,* vol. 19, no. 9, p. 093010, 2017.
[http://dx.doi.org/10.1088/1367-2630/aa8742]

[7]   "Cornell Electron Storage Ring", *CLASSE: CESR. Cornell laboratory for accelerator-based sciences and education,* 2014. Available from: http://www.lepp.cornell.edu/Research/CESR/WebHome.html

[8]   J. Kevorkian, and J.D. Cole, Perturbation methods in applied mathematics.*Applied Mathematical Sciences.,* vol. 34. Springer: Waltham, MA, 1981.

[9]   R.H. Rand, *Lecture Notes in Nonlinear Vibrations.,* Published on-line by The Internet-First University Press, 2012. Available from: http://ecommons.library.cornell.edu/handle/1813/28989

[10]   MATLAB v.7.5 by Mathworks; applet pplane7.m by Polking, J. C , Rice University, Department of Mathematics, Available from: http://math.rice.edu/□dfield/dfpp.html